



1 **A novel multi proxy approach reveals that the millennial old ice cap on**
2 **Weißseespitze, Eastern Alps, has preserved its chemical and isotopic signatures**
3 **despite ongoing ice loss**
4

5 **Azzurra Spagnesi^{1,2}, Pascal Bohleber^{1,3}, Elena Barbaro², Matteo Feltracco¹, Fabrizio De Blasi^{1,2},**
6 **Giuliano Dreossi^{1,2}, Martin Stocker-Waldhuber³, Daniela Festi⁴, Jacopo Gabrieli², Andrea Gambaro^{1,2},**
7 **Andrea Fischer³, Carlo Barbante^{1,2}**

8
9 ¹ Department of Environmental Sciences, Informatics and Statistics, Ca' Foscari University of Venice, Venice, Italy

10 ² CNR-Institute of Polar Sciences (ISP-CNR), 155 Via Torino, 30170 Mestre, Italy

11 ³ Institute for Interdisciplinary Mountain Research of the Austrian Academy of Sciences, Innrain 25/3, 6020 Innsbruck,
12 Austria

13 ⁴ GeoSphere Austria, Neulinggasse 38, 1030 Vienna, Austria
14

15 **Correspondence:** Azzurra Spagnesi (azzurra.spagnesi@unive.it)
16

17 **Abstract**
18

19 From the 1970s to the early 2000s, Alpine ice core research focused on a few suitable drilling sites at high
20 elevation in the Western European Alps, assuming that the counterparts at lower elevation in the eastern sector
21 are unsuitable for paleoenvironmental studies, due to the presence of melting and temperate basal conditions.
22 Since then, it has been demonstrated that even in the Eastern Alpine range, below 4000 m a.s.l., cold ice frozen
23 to bedrock can exist. In fact, millennial-old ice has been found at some locations, such as at the Weißseespitze
24 (WSS) summit ice cap (Ötztal Alps, 3499 m a.s.l.), where about 6 kyrs appear locked into 10 m of ice. In this
25 work, we present a full profile of the stable water isotopes ($\delta^{18}\text{O}$, $\delta^2\text{H}$), major ions (Na^+ , Cl^- , Br^- , K^+ , Mg^{2+} ,
26 Ca^{2+} , NO_3^- , SO_4^{2-} , NH_4^+ , MSA^-), levoglucosan, and microcharcoal for two parallel ice cores drilled at the
27 Weißseespitze cap. We find that, despite the ongoing ice loss, the chemical and isotopic signatures appear
28 preserved, and may potentially offer an untapped climatic record. This is especially noteworthy considering
29 that chemical signals of other archives at similar locations have been partially or full corrupted by meltwater
30 (i.e., Silvretta glacier, Grand Combin glacier, Ortles glacier). In addition, the impurity concentration near the
31 surface shows no signs of anthropogenic contamination at WSS, which constrains the age at the surface to falls
32 within the pre-industrial age.

33
34 **1. Introduction**

35 European Alpine glaciers represent unique targets for ice core studies focusing on reconstructing
36 environmental and climatic conditions in the Holocene. Since its beginning, a primary aim of ice core research
37 in the Alps was retrieving continuous stratigraphic climate records, which restricted it to glaciers without
38 significant melting on the surface throughout the year. In this strict view, only few suitable drilling sites exist
39 as they are mostly confined to above 4000 m altitude and hence located in the Western Alps, which have been
40 exploited in numerous successful studies over the past four decades (Bohleber, 2019, and references therein).
41 Following evidence that old ice may also exist in the Eastern Alps and at elevations below 4000 m (Haeberli
42 et al., 2004), new efforts targeted the either direct access to the ice at the glacier base (Bohleber et al., 2018)
43 or the drilling of ice cores at both temperate (Pavlova et al., 2015; Festi et al., 2017), partially temperate but



44 cold-based (Gabielli et al., 2016) and predominantly cold ice sites (Bohleber et al., 2020a). In concert with
45 state-of-the-art radiocarbon ice dating (Uglietti et al., 2016; Hoffmann et al., 2018), the access to the stagnant
46 cold ice at the glacier base revealed that millennial-old ice is still preserved even if the remaining thickness is
47 only around 10 m or less, adding important information for reconstructing the Holocene neoglaciation history
48 of the Alps (Bohleber et al., 2020a). Retrieving the paleoclimate and environmental information potentially
49 stored in these ice cores' chemical and isotopic stratigraphy means facing additional complexity to what it is
50 already known for the "classical" ice core targets in the Western Alps (Wagenbach et al., 2012). First, due to
51 ongoing and prolonged mass loss also the age of the ice at the surface becomes an unknown parameter that
52 requires separate dating efforts with innovative approaches (Festi et al., 2021). Second, due to their lower
53 elevation, these sites are typically much closer to the equilibrium line altitude of the glacier, making them not
54 only more vulnerable to present warming conditions but also a potential sensitive indicator of past climate
55 shifts impacting their energy and mass balance. In fact, prolonged periods of stagnation or mass loss may have
56 occurred and resulted in stratigraphic discontinuities at such sites (Fischer et al., 2022). Third, meltwater
57 percolation can corrupt and ultimately erase completely the chemical and isotopic information in the
58 stratigraphy, although the degree of the disturbances may depend on the impurity species and the degree of
59 percolation (Avak et al., 2018; Eichler et al., 2001).

60 Here we present recent progress in evaluating these challenges for the new ice cores drilled at the
61 Weißseespitze cap, Eastern Alps (WSS). We use for this purpose profiles of the stable water isotopes ($\delta^2\text{H}$ and
62 $\delta^{18}\text{O}$), major ion chemistry as well as a full profile of microcharcoal and levoglucosan. The latter represents a
63 novelty for ice core studies over the alpine range, since only a preliminary work at Col du Dome is currently
64 available (Legrand et al., 2007). Levoglucosan was measured on the WSS ice core to investigate if evidence
65 of past biomass burning events could be detected, since levoglucosan is particularly useful when source and
66 deposition sites are close to each other (Alves et al., 2017).

67

68 **2. Methods**

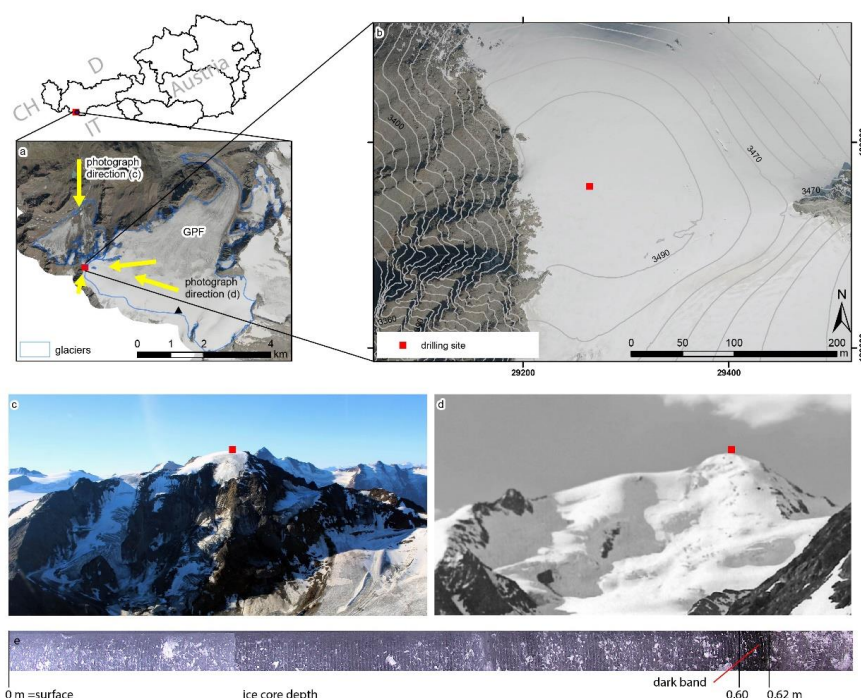
69

70 **2.1 Glaciological settings of the ice core drilling site at Weißseespitze**

71 The Weißseespitze ice cap (around 3500 m a.s.l.) covers the top sections of Gepatschferner glacier in the
72 Austrian Alps (Fig. 1a,b), located only 12 km from the famous Tyrolean Iceman find site. Its limited ice
73 thickness combined with a dome-shaped glacier geometry entails minimal to no ice flow, confirmed by
74 differential GPS measurements at stakes in 2018 and 2019. Historical photographs dating back to about 1888,
75 maps and digital elevation models reveal that the ice body today is the remnant of a much larger ice cap
76 diminished by prolonged ice loss (Fig. 1c,d). Despite the prolonged ablation, englacial borehole temperatures
77 remained permanently sub-zero at 1 m below surface, with -3°C at 9 m of depth (Fischer et al., 2022). A first
78 ice core was drilled to bedrock (11 m in total, including about 1 m of snow cover but no firn) at the ice divide
79 with nearly flat bed conditions in March 2019. An additional parallel core (8.7 m of depth to bedrock) was
80 drilled at the same location in March 2021. The few visible layers of refrozen meltwater in the cores indicate



81 that there was only limited occasional melt at this site when the ice formed. The main part of the ice cores
82 includes bubble-rich glacier ice, the likely result of dry metamorphosis of snow (Fig. 1e). Initial analysis
83 supported this view, e.g., by stable oxygen and hydrogen ratios, exhibiting a range typical for the seasonal
84 variation in snow at this altitude, and no systematic deviation from the meteoric water line (Bohleber et al.,
85 2020a). The 2019 surface at WSS is older than 1963, indicated by the absence of elevated tritium levels within
86 the first 4 m of the core. The aerosol-based micro-¹⁴C dating indicated a maximum age of (5.884 ± 0.739) ka
87 cal BP just above the bed. Further details on the glaciological settings have already been described in former
88 studies (Bohleber et al., 2020a; Fischer et al., 2022).



89
90
91 **Figure 1.** The ice core drilling site at the summit of the Weißseespitze ice cap (a, b). Datenquelle: Land Tirol
92 - data.tirol.gv.at. Panoramic view of the Weißseespitze ice cap in 2019 (c), and 1930 (d). One of the ice cores
93 taken in 2019 (e).

94 2.2 Ice core processing and analysis

95
96 To prepare for Continuous Flow Analysis (CFA) at Ca'Foscari University of Venice, the 2019 core was
97 processed to obtain 23 ice sticks (*bags*) with 32 x 32 mm sections. Only the top 8.5 m were considered suitable
98 for the analysis, given the high concentration of visible debris at the bottom. The ice was cut with a modified
99 commercial band saw, and refined with a decontaminated stainless-steel blade over a polyethylene tabletop
100 accessorized with guide rails for cutting. The table, rails, and the blade were carefully cleaned with acetone
101
102



103 and methanol to remove contamination before every use. All the exposed ice surfaces were rapidly scraped
104 with a stainless-steel knife cleaned with 0.1 % ultra-pure HNO₃ (Romil, Cambridge, UK). This knife was used
105 to remove the outer thin contaminated ice layer, and more mass was scraped from the two base surfaces which
106 were to be placed on the melting head. Several mm of ice from each end were removed by using a second
107 clean knife to ensure perfect contact to the melting head surface. The sections were stored in clean PTFE bags
108 until the analyses conducted with the novel set-up of the Continuous Flow Analysis system realized at Ca'
109 Foscari, in collaboration with the National Research Council - Institute of Polar Science (CNR-ISP). This
110 technique allows to continuously measure insoluble dust particles (1 acquisition sec⁻¹) and levoglucosan (1 cm
111 of resolution) within the meltwater stream, while sets of discrete samples (2.6 cm of ice depth equivalent per
112 sample) were reserved for the off-line analysis of water stable isotopes and major ions, conducted via Cavity
113 Ring-Down Spectroscopy (CRDS, Picarro inc.), and Ion Chromatrography (IC), respectively. The overall CFA
114 system coupled with Fast Liquid Chromatography tandem Mass Spectrometry (FLC – MS/MS), is illustrated
115 in Barbaro et al. (2022), while the optimization of the method for levoglucosan continuous measurements is
116 presented in Spagnesi et al. (2023).

117 In order to investigate the localization of the impurities in the ice matrix and their potential removal through
118 meltwater percolation under temperate conditions, exemplary sections were analysed at the University of
119 Venice by 2D chemical imaging with laser ablation inductively-coupled plasma mass spectrometry (LA-ICP-
120 MS). The LA-ICP-MS set-up comprised an Analyte Excite ArF excimer 193 nm laser (Teledyne CETAC
121 Photon Machines) and an iCAP-RQ quadrupole ICP-MS (Thermo Scientific), connected via a rapid aerosol
122 transfer line for fast washout. Samples surfaces are decontaminated with ceramic ZrO₂ blades (American
123 Cutting Edge, USA), and the sample is then placed on a cryogenic sample holder. A glycol-water mixture (-
124 35°C) is used to cool the sample surface to -23 +/-2°C which is further cleaned by preablation with an 80 x 80
125 µm square spot before each measurement. Further details are described in Bohleber et al. (2020)b.

126 Sample stripes of about 8 x 2 x 1 cm were cut from bags 2 and 18, at depths of 0.08 – 0.10 and 6.25 – 6.75 m,
127 respectively. Images were recorded using a 40 micron spot over areas that showed visual evidence of grains
128 and grain boundaries. Due to the comparatively large grains in bag 18, only one grain boundary was present
129 within the image. Analytes were Na, Mg, Al and Fe in order to consider species with mostly soluble (Na, Mg)
130 as well as insoluble (Al, Fe) behaviour.

131 The 8.4 m long ice core drilled in 2021 was cut in 106 continuous samples at 10 cm resolution from the surface
132 to 6.6 m of depth, and at 5 cm resolution from 6.6 m to the bottom. The ice was cut with a modified commercial
133 band saw. Samples were stored frozen in plastic bags and sent frozen to the Palynological Laboratory at Milano
134 Bicocca University for microfossils extraction (including microcharcoal) and preparation. Decontamination
135 was performed using fridge-cooled distilled water and left to melt covered at room temperature. Sample
136 volume was measured and samples were then filtered with a 7-µm filter to concentrate the microfossils (pollen,
137 spores, microcharcoal and other non-pollen-palynomorphs). The so concentrated samples underwent chemical
138 digestion according to Festi et al. (2019). Microscopy slides were prepared in the Milano laboratory and
139 analysed at the Institute for Interdisciplinary Mountain Research of the Austrian Academy of Sciences using



140 a Motic BA310 light microscope. Microcharcoal particles ($> 7 \mu\text{m}$) were quantified along with pollen grains
 141 as usual in pollen analyses. For each sample, the complete content was analysed. In this work, we present the
 142 microcharcoal record obtained for the core.

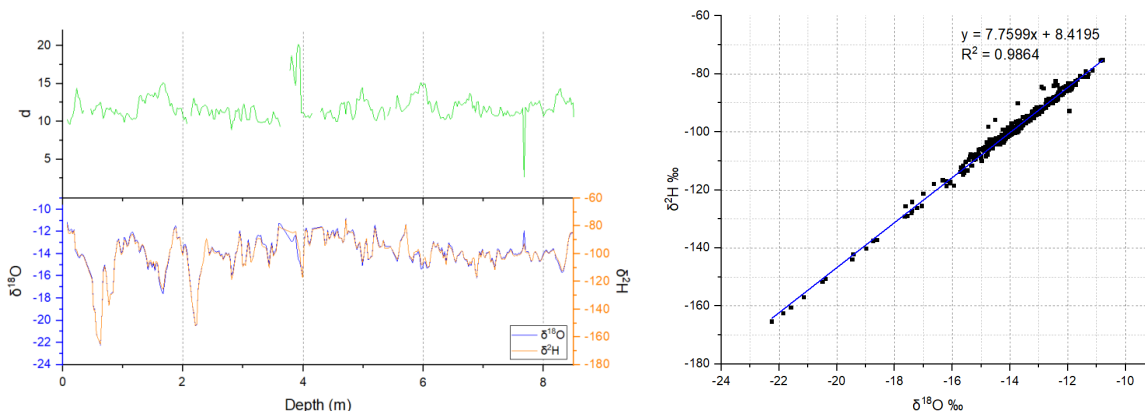
143 3. Results

144 3.1 Water stable isotopes

145 Water stable isotopes ($\delta^{18}\text{O}$, $\delta^2\text{H}$) and deuterium excess were measured in discrete samples, resulting in the
 146 depth profiles shown in Fig. 2. The upper part of the core, ranging from 0 to roughly -2.30 m of depth, is
 147 characterized by distinct decimeter-scale variability over several permil in $\delta^{18}\text{O}$. We find two marked minima
 148 ($\delta^{18}\text{O}$: -22 ‰, -20 ‰; $\delta^2\text{H}$: -165 ‰, -152 ‰) located at -0.63 m and -2.27 m of depth, respectively, with
 149 isotopic signals similar to higher elevation Alpine sites (Wagenbach et al., 2012; Bohleber et al., 2013). By
 150 comparison, the deeper part of the core below 6 m only shows minor variability around a stable mean (-14 ‰
 151 ± 1 ‰). However, there is clear decimeter-scale variability found over the entire depth range. Overall, the
 152 deuterium excess record (d) does not show any clear trend, with values ranging between 10 and 15, similarly
 153 to what observed by Fröhlich et al. (2008) for stations located north and south of the main ridge of the Austrian
 154 Alps. Only one marked maximum, located around 4 m of depth, deviates from this general trend: this peak
 155 corresponds to a minimum in $\delta^{18}\text{O}$ and $\delta^2\text{H}$; other negatively-correlated values between d and $\delta^{18}\text{O}$ ($\delta^2\text{H}$) can
 156 be observed at -1.67, -4.99, -5.96 and -8.28 m of depth.

158 The slope in the co-isotopic plot is 7.76 ± 0.05 , with a R^2 for the linear fit of 0.9864. This value is very close
 159 with previous results obtained by Bohleber et al. (2020), for the same drill site, albeit at coarser depth
 160 resolution. Notably, the slope reveals no systematic deviation from the local meteoric water line calculated on
 161 the Villacher GNIP station monthly precipitation data between 1973 and 2002: $\delta\text{D}=8.09\delta^{18}\text{O}+12.48$ (IAEA,
 162 2023).

163



164
 165
 166
 167
 168

Figure 2. Deuterium excess (d), $\delta^{18}\text{O}$ and $\delta^2\text{H}$ profiles (‰) along the WSS ice core (left), and $\delta^{18}\text{O}/\delta^2\text{H}$ linear regression (right).



3.2 Major ions chemistry, levoglucosan and insoluble dust particles

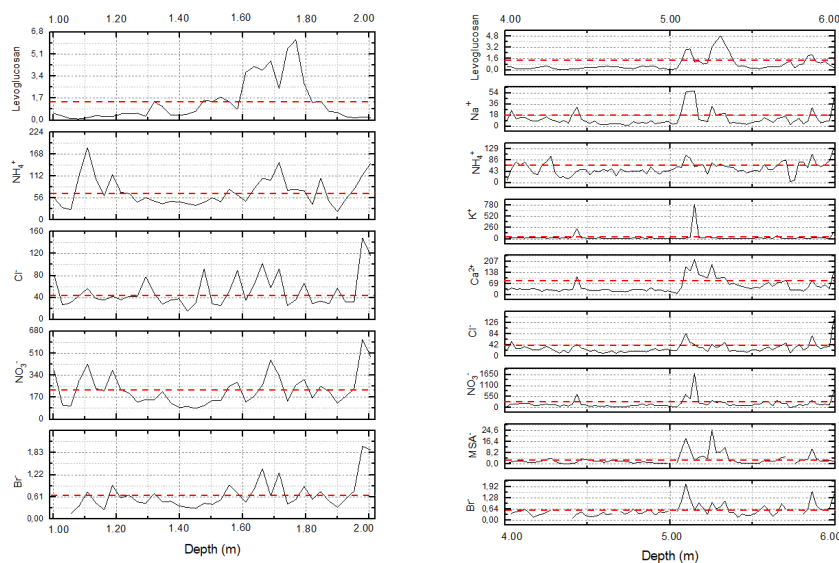
169
170
171
172
173
174
175
176
177
178
179
180
181
182
183
184
185
186
187
188
189
190
191
192
193
194
195
196
197
198
199
200
201
202
203
204
205
206

The obtained levoglucosan profile shows concentration ranges between 0.07 and 51.07 ng mL⁻¹, with a major peak found at ~ 6.40 m (Fig. 3). To investigate if this outstanding feature is connected to other proxy data, the size-distribution of the insoluble dust particles was used to calculate a Fine Particle Percentage (FPP) along the whole depth, summing the number of particles detected between 0.8 and 3.9 μm. The threshold of 3.9 μm was chosen according to Wagenbach and Geis (1989), as an indicator for the median particle diameter of Saharan dust, albeit at high Alpine locations. About 85.2 % ca. of particles are below 4 μm in size (ø < 4 μm), almost equally distributed along the ice core, with a decrease of 4 % ca. for FPP observed for the deepest section (from 6 m to 8.5 m).

Cationic (Na⁺, NH₄⁺, K⁺, Mg²⁺, Ca²⁺), and anionic species (Cl⁻, NO₃⁻, SO₄²⁻, Br⁻, MSA⁻) were analysed within the discrete samples collected during the melting campaign. The mean concentrations, SD, minimum, maximum, and median values of all the ionic compounds and water stable isotopes were computed over the whole core depth and the upper 1 m separately, but showing no significant differences between the two sets for NH₄⁺, K⁺, Ca²⁺, NO₃⁻, and Br⁻ (Table 1). The overall chemical composition is dominated by nitrate (NO₃⁻, 37 %), sulphate (SO₄²⁻, 23 %), calcium (Ca²⁺, 12 %), and ammonium (NH₄⁺, 11 %). Minor contributions were reported for Cl⁻, K⁺, Na⁺, and Mg²⁺, respectively, quantified as 6.93 %, 3.82 %, 3.05 %, and 2.21 %, while MSA⁻ and Br⁻ accounted for 0.58 % and 0.09 % of the total ionic species. The ionic balance was evaluated considering the ionic concentrations in terms of equivalent, in order to evaluate the degree of neutralization. The difference between the sum of anions and the sum of cations is always around ± 5 % over the whole profile of the core. The prevalent cations/anions ratio > 1 indicates a limited defect of anions (Fig. S2), likely related to the carbonates (CO₃²⁻), which were not analysed in this work due to instrumental limits. Figure S2 displays some values < 1, which can suggest the presence of cations deficit, likely due to the presence of H⁺.

Regarding the localization of the impurities as investigated by LA-ICP-MS, Fig. 4 shows the near surface sample (WSS bag 02), and the examples of Na, Mg and Al in a separate colour channel. All elements (including Fe and Sr) are predominantly localized at grain boundaries, which are visible in Fig. 4 as lines of bright intensity. The second sample from bag 18 in shown in the supplement, with the same basic finding (Fig.

S3).





207
208
209
210
211
212
213
214
215
216
217
218
219
220
221
222
223
224
225

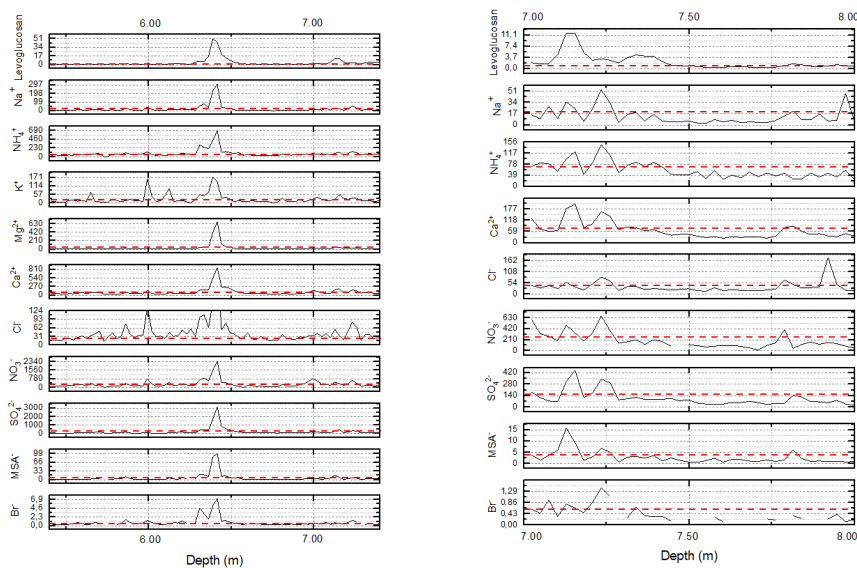


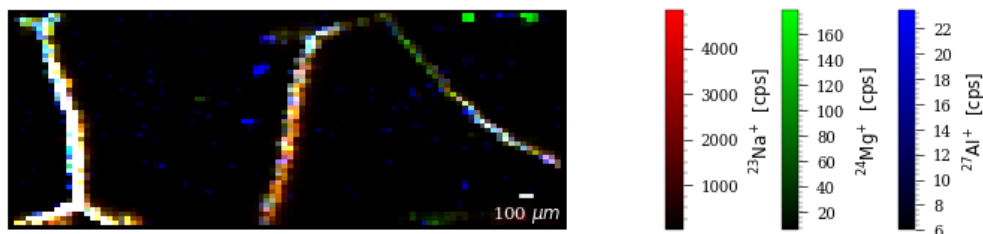
Figure 3. Zoom in from Fig. 4 at: (1) 1.60-1.90 m, (2) 5.00-5.50 m, (3) 6.40 m, and (4) 7.10-7.20 m of depth.

Concentrations on y-axes are expressed in ng mL^{-1} . Red dashed lines indicate mean values.

Table 1. Ionic compound and water stable isotopes (WSI) average, min, max, and median values for the whole core depth and the upper 1 m (concentrations are expressed in ng mL^{-1}).

Ionic compound and WSI	whole core				upper 1 m			
	Average \pm SD	Min	Max	Median	Average \pm SD	Min	Max	Median
Na ⁺	18 \pm 29	1.34	305	9.36	39 \pm 40	4.90	166	20
NH ₄ ⁺	67 \pm 64	2.87	685	52	74 \pm 78	12	440	56
K ⁺	23 \pm 52	1.59	802	13	30 \pm 28	2.38	102	17
Mg ²⁺	14 \pm 45	1.85	673	6.60	5.42 \pm 1.43	2.11	8.72	5.28
Ca ²⁺	73 \pm 74	11	866	53	75 \pm 27	26	150	69
Cl ⁻	42 \pm 37	11	291	30	79 \pm 62	21	248	46
NO ₃ ⁻	226 \pm 245	6.67	2371	154	204 \pm 95	89	426	190
SO ₄ ²⁻	144 \pm 266	7.09	3119	79	97 \pm 80	32	363	68
MSA ⁻	3.73 \pm 8.39	0.15	99	1.94	0.91 \pm 0.69	0.15	2.21	0.59
Br ⁻	0.62 \pm 0.66	0.07	7.11	0.47	0.49 \pm 0.25	0.13	1.07	0.47
$\delta^{18}\text{O}$ ‰	-14 \pm 1	-15	-13	-14	-15 \pm 3	-18	-12	-14
$\delta^2\text{H}$ ‰	-100 \pm 13	-113	-87	-99	-112 \pm 24	-136	-88	-102

226
227



228
229 **Figure 4.** WSS ice core sample from bag 2. The LA-ICP-MS image consists of 50 lines measured with a 40 micron spot
230 and shows Na, Mg, Al in red, green and blue color scale, respectively for an area of 2 x 5 mm. All elements are found
231 mostly co-localized at grain boundaries (bright lines), while Al and Mg also form some isolated spots.

232
233

3.3 Microcharcoal

234 Microcharcoal concentration in the core ranges from 0 to 26.4 particles per mL (Fig. 5). Only 23 over 106
235 samples contained no microcharcoal and in the 8.4 m long profile, several peaks can be identified. The most
236 prominent one is found 8 cm below the surface of the core, from 8 to 28 cm of depth and reaches the maximum
237 concentration of 26.4 particles mL⁻¹. Applying a smoothing, three further composite peaks stand out at 3.5-4
238 m, 4.7-5.2 m and 5.6-6.2 m of depth.

239
240
241
242
243

4. Discussion

4.1 A preserved chemical and isotopic record

244 The fact that no deviation from the meteoric water line is indicated in the co-isotopic plot suggests the absence
245 of substantial melting and refreezing processes on the cm-scale (Craig, 1961), thus constituting an analogue
246 situation to what was previously observed for other cold-based alpine summit sites (Bohleber et al., 2018;
247 Bohleber et al., 2020a). This is also consistent with the fact that no clear visual evidence of refrozen ice
248 manifesting as transparent bubble-free layers was found in visual analysis of this ice core. Throughout the
249 entire record, notably including the near-surface layers, we find distinct variability in the chemical and isotopic
250 signals obtained from the ice core. We can further exclude substantial percolation of meltwater, as this would
251 have likely led to the continuous removal of impurities by gradual washing out, hence reducing and eventually
252 removing any variability (Pavlova et al., 2015; Schotterer et al., 2004). This is consistent with what we have
253 found in the exemplary LA-ICP-MS maps, which show a typical degree of impurity localization at grain
254 boundaries previously observed in cold polar ice conditions (Souchez and Jouzel, 1984). We thus conclude
255 that, despite the intense ablation which is acting at the surface of the Weißseespitze summit ice cap today, the
256 cold ice remains mostly impermeable to meltwater which must be running off along the snow/firn layers. This
257 is backed by the sub-zero temperatures measured inside the boreholes (Bohleber et al., 2020a; Fischer et al.,
258 2022). As a result of these conditions, the ice contains preserved isotopic and chemical signals observed along
259 the ice core depth. This is not to be expected a-priori considering what was revealed for other Alpine sites,
260 such as the nearby Ortles (Gabielli et al., 2016), the Silvretta glacier (Pavlova et al., 2015; Steinlin et al.,



261 2015) or the Grand Combin glacier (Huber et al., 2022), where the archives have been partially lost, and flat
262 signals (i.e., Silvretta glacier) or depleted impurity concentrations (i.e., Grand Combin) have been recorded.
263 Because only the lower, older and thinned ice layers remain today at the Weißseespitze site, any seasonal
264 variations of the isotopic signal is not detectable at the present resolution. Regarding the outstanding peak in
265 the deuterium-excess profile at around 4 m of depth, we find no evidence of an instrumental origin, hence this
266 feature may be indicative of a change at the moisture source (Fröhlich et al., 2002). In particular, it can be
267 hypothesized that this indicates a period of exceptional recycling of continental moisture or moisture masses
268 formed over the Mediterranean basin (Fröhlich et al., 2008).

269

270

4.2 Old ice at the surface and significance of the average impurity concentrations

271 Apart from the fact that the impurity record appears overall undisturbed, it is noteworthy that the near-surface
272 layers show no distinct difference in concentration levels with respect to the rest of the core (Table 1). Within
273 the last 80-100 years, a distinct increase in most impurity species is observed in other Alpine ice cores due to
274 anthropogenic emissions, in particular for NO_3^- , SO_4^{2-} , and NH_4^+ (Bohleber, 2019; Wagenbaach et al., 2012;
275 Schwikowski et al., 1999a; Schwikowski et al., 1999b; Preunkert et al., 2003). This indicates that the current
276 surface at WSS is not only missing the ^3H bomb horizon conventionally associated with the year 1963 as
277 detected previously by Bohleber et al. (2020), but that the present surface is in fact significantly older than
278 1963 and falls within the pre-industrial time period.

279 Notably, the $\text{SO}_4^{2-}/\text{Ca}^{2+}$ ratio calculated for the upper 1 m of the core gives a mean molar ratio of 0.56. This
280 is comparable to the ratio of 0.59 computed by Wagenbach et al. (1996) for the pre-industrial (pre-1930)
281 period, which points towards a similar contribution of Saharan dust to the snow chemistry at WSS. Correlation
282 analysis using the non-parametrical Spearman correlation matrix reveals that all ions positively correlate with
283 each other (significance level 0.05, Fig. S1), which also holds for their trend variability. Considering that most
284 impurities feature a distinct seasonality at high alpine sites due to a seasonal contrast in vertical mixing strength
285 of the atmosphere (Preunkert et al., 2001), systematic changes in the seasonality of snow deposition is a prime
286 candidate to introduce such an apparent coupling among different ionic species with different emission sources
287 (Wagenbach et al., 2012).

288 A more detailed interpretation of the impurity record and comparison with other Alpine ice core records would
289 benefit greatly from constraining the seasonal bias in net snow deposition, which is to be expected at an
290 exposed summit site. Monitoring today's conditions at the surface is unsuitable for this purpose because it is
291 dominated by ablation all throughout the year. As a crude attempt at investigating potential seasonal biases in
292 snow deposition, we took a closer look at the average levels in $\delta^{18}\text{O}$, which contains a known clear seasonal
293 cycle in precipitation. The closest nearby meteorological weather station is located at Villacher Alpe (VA, Lat.
294 46.60 N, Long. 13.67 E, 2156 m a.s.l.), for which also data from the Global Network on Isotopes in
295 Precipitation (GNIP) are available for the 1973-2002 period (IAEA, 2023). The average seasonal cycle was
296 calculated for this time period and subsampled for all seasons. Results were corrected for the elevation
297 difference (using $-0.09\text{‰}/100\text{ m}$, as reported in Siegenthaler and Oeschger, 1980), obtaining a VA $\delta^{18}\text{O}$ fall

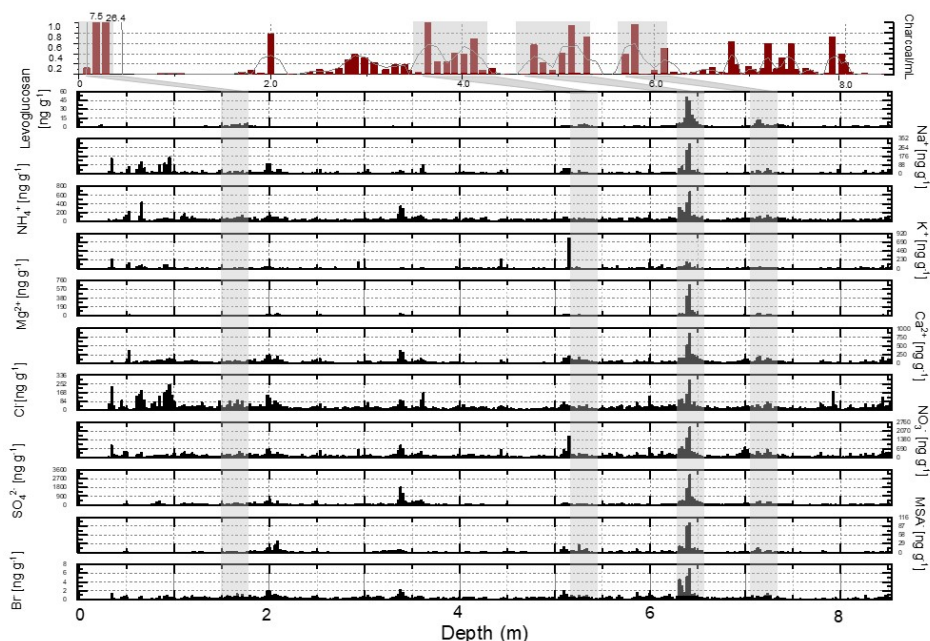


298 average value of -14.05%, which is close to the average value over the entire WSS record, being -13.98 %
299 (Table S1). This tentatively indicates that snow preservation is neither restricted to the winter nor the summer,
300 but is likely a mix. However, this comparison suffers again from the fact that the two-time intervals do not
301 overlap due to the lack of the 1973-2002 time period in the WSS core. Acknowledging the present uncertainty
302 in the snow deposition bias, the impurity levels can indicate the general pre-industrial background in
303 precipitation for this region.

304

305 4.3 Outstanding peaks in levoglucosan, microcharcoal and impurities

306 In the core of 2019 levoglucosan and chemistry peaks are visible at 1.60-1.90 m, 5.00-5.50 m, 6.40 m, and
307 7.10-7.20 m of depth, respectively (grey bars in Fig. 5, and zoom-ins Fig. 3). The third event at 6.40 m showed
308 a visual correspondence with all the investigated ions. At the same time, four outstanding periods are also
309 present in the microcharcoal data analysed in the 2021 core. This core was drilled at about 10 m distance from
310 the 2019 core. Notably, the measured ice ablation at the surface shows a strong gradient on a very short distance
311 between the stakes placed at the drilling sites, with up to 110 cm of ablation within the period 2019-2021.
312 Considering these surface changes and that both levoglucosan and microcharcoal are proxies of biomass
313 burning, it appears plausible to match the near-surface microcharcoal peak in 2021 with the first levoglucosan
314 peak of the 2019 core. The striking correspondence of the four levoglucosan peaks with the four main
315 microcharcoal concentration peaks (Fig. 5) supports the hypothesis that at least four main fire activity phases
316 are recorded in the WSS ice record.



317



318 **Figure 5.** Full levoglucosan and chemistry profiles along the whole WSS longest core depth drilled in 2019.
319 Concentrations on y-axes are expressed in ng mL^{-1} . Grey bars indicate corresponding peaks between levoglucosan and
320 major ions. Microcharcoal/mL profile along the 8.4 m length WSS core drilled in 2021 is presented in the above graph
321 with brown bars.

322

323 **5. Conclusion**

324 The Weißseespitze summit ice cap has preserved the chemical and isotopic signature embedded in the ice,
325 despite the intense ice loss affecting the glacier's surface today. Indeed, the surface melting does not appear to
326 dominantly affect the remaining ice on the cm-scale, as indicated by a co-isotopic slope close to global
327 meteoric water line. The chemical signal in the upper meters of the ice does not show any evidence of the
328 anthropogenic increase during the 20th century known from other ice core. In particular, nitrates, sulphates,
329 and ammonium present pre-industrial concentrations. These results corroborate the previous age constraints
330 from ^3H , showing the absence of the 1963 bomb horizon at the surface, but also indicate that today's surface
331 is much older and falls within the pre-industrial ear. The lack of temporal overlap between the WSS record
332 and instrumental data hampers constraining the seasonal representativeness and snow deposition bias so far.
333 However, four major peaks have been recognised standing out for levoglucosan but also other impurity species.
334 Based on the absence of evidence for disturbances by melting and refreezing, these events may stem from
335 either singular biomass burning events or a surface with prolonged exposure to the atmosphere during a hiatus.
336 With a future more robust estimate of the age-depth relation at WSS, comparisons with similar ice core alpine
337 records (e.g., ice cores from Alto dell'Ortles) or other natural archives (e.g., peatbogs), may offer new valuable
338 insights regarding the regional significance of these outstanding horizons.

339

340 **Data availability**

341

342 Data will be made available on request.

343

344

345 **Author contributions**

346 Conceptualization: Azzurra Spagnesi, Pascal Bohleber, Elena Barbaro; Methodology: Azzurra Spagnesi, Elena
347 Barbaro, Matteo Feltracco, Pascal Bohleber, Fabrizio De Blasi, Giuliano Dreossi, Jacopo Gabrieli; Formal
348 analysis and investigation: Azzurra Spagnesi, Elena Barbaro, Matteo Feltracco, Fabrizio De Blasi, Giuliano
349 Dreossi, Pascal Bohleber, Daniela Festi; Writing - original draft preparation: Azzurra Spagnesi, Pascal
350 Bohleber; Writing - review and editing: Azzurra Spagnesi, Pascal Bohleber, Andrea Fischer, Elena Barbaro,
351 Matteo Feltracco, Giuliano Dreossi, Daniela Festi, Martin Stocker-Waldhuber, Jacopo Gabrieli, Andrea
352 Gambaro, Carlo Barbante; Supervision: Jacopo Gabrieli, Andrea Fischer, Andrea Gambaro, Carlo Barbante.

353

354 **Competing interests:** The authors declare that they have no known competing financial interests or personal
355 relationships that could have appeared to influence the work reported in this paper.

356



357 **Acknowledgments**

358

359 This research was funded in part by the Austrian Science Fund (FWF) [I 5246-N and P34399-N]. For the
360 purpose of open access, the author has applied a CC BY public copyright licence to any Author Accepted
361 Manuscript version arising from this submission.

362 Pascal Bohleber gratefully acknowledges funding from the European Union's Horizon 2020 research and
363 innovation program under the Marie Skłodowska-Curie grant agreement no. 101018266.

364

365

366

367

References

368

369 Alves, C.A., Vicente, E.D., Rocha, S. and Vicente, A.M.: Organic tracers in aerosols from the residential
370 combustion of pellets and agro-fuels, air quality, *Atmos. Health*, 10, 37-45,
371 <https://doi.org/10.1007/s11869-016-0406-3>, 2017.

372 Avak, S.E., Schwikowski, M. and Eichler, A.: Impact and implications of meltwater percolation on trace
373 element records observed in a high-Alpine ice core, *J. Glaciol.*, 64(248), 877-886,
374 <https://doi.org/10.1017/jog.2018.74>, 2018.

375 Barbaro, E., Feltracco, M., Spagnesi, A., Dallo, F., Gabrieli, J., De Blasi, F., Zannoni, D., Cairns, W.R.L.,
376 Gambaro, A. and Barbante, C.: Fast liquid chromatography coupled with tandem mass
377 spectrometry for vanillic and syringic acids analysis in ice cores, *Anal. Chem.*, 94(13), 5344-5351,
378 <https://doi.org/10.1021/acs.analchem.1c05412>, 2022.

379 Bohleber, P., Wagenbach, D., Schöner, W., and Böhm, R.: To what extent do water isotope records from
380 low accumulation Alpine ice cores reproduce instrumental temperature series?, *Tellus B*, 65,
381 20148, <http://dx.doi.org/10.3402/tellusb.v65i0.20148>, 2013.

382 Bohleber, P., Hoffmann, H., Kerch, J., Sold, L. and Fischer, A.: Investigating cold based summit glaciers
383 through direct access to the glacier base: a case study constraining the maximum age of Chli Titlis
384 glacier, Switzerland, *The Cryosphere*, 12(1), 401-412, <https://doi.org/10.5194/tc-12-401-2018>,
385 2018.

386 Bohleber, P.: Alpine ice cores as climate and environmental archives, in: *Oxford Research Encyclopedia*
387 *of Climate Science*, edited by: Oxford University Press,
388 <https://doi.org/10.1093/acrefore/9780190228620.013.743>, 2019.

389 Bohleber, P., Schwikowski, M., Stocker-Waldhuber, M., Fang, L. and Fischer, A.: New glacier evidence
390 for ice-free summits during the life of the Tyrolean Iceman, *Sci. Rep.*, 10, 20513,
391 <https://doi.org/10.1038/s41598-020-77518-9>, 2020a.

392 Bohleber, P., Roman, M., Šála, M., and Barbante, C.: Imaging the impurity distribution in glacier ice cores
393 with LA-ICP-MS, *JAAS*, 35(10), 2204-2212, <https://doi.org/10.1039/D0JA00170H>, 2020b.

394 Craig, H.: Isotopic variations in meteoric waters, *Science*, 133, 1702-1703,
395 <https://doi.org/10.1126/science.133.3465.1702>, 1961.



- 396 Eichler, A., Schwikowski, M. and Gäggeler, H.W.: Meltwater-induced relocation of chemical species in
397 Alpine firn, *Tellus*, 53B, 192-203, <https://doi.org/10.3402/tellusb.v53i2.16575>, 2001.
- 398 Festi, D., Carturan, L., Kofler, W., dalla Fontana, G., de Blasi, F., Cazorzi, F., Bucher, E., Mair, V.,
399 Gabrielli, P. and Oeggl, K.: Linking pollen deposition, snow accumulation and isotopic
400 composition on the Alto dell'Ortles glacier (South Tyrol, Italy) for sub-seasonal dating of a firn
401 temperate core, *The Cryosphere*, 11, 937-948, <https://doi.org/10.5194/tc-11-937-2017>, 2017.
- 402 Festi, D., Kofler, W., and Oeggl, K.: Comments on Brugger and others (2018) 'A quantitative comparison
403 of microfossil extraction methods from ice cores,' *J. Glaciol.*, 65, 344-346,
404 <https://doi.org/10.1017/jog.2019.10>, 2019.
- 405 Festi, D., Schwikowski, M., Maggi, V., Oeggl, K. and Jenk, T.M.: Significant mass loss in the accumulation
406 area of the Adamello glacier indicated by the chronology of a 46 m ice core, *The Cryosphere*, 15,
407 4135-4143, <https://doi.org/10.5194/tc-15-4135-2021>, 2021.
- 408 Fischer, A., Stocker-Waldhuber, M., Frey, M. and Bohleber, P.: Contemporary mass balance on a cold
409 Eastern Alpine ice cap as a potential link to the Holocene climate, *Sci. Rep.*, 12(1331), 1-13,
410 <https://doi.org/10.1038/s41598-021-04699-2>, 2022.
- 411 Fröhlich, K., Gibson, J.J., and Aggarwal, P.K.: Deuterium excess in precipitation and its climatological
412 significance, (IAEA-CSP--13/P), International Atomic Energy Agency (IAEA), 2002.
- 413 Fröhlich, K., Kralik, M., Papesch, W., Rank, D., Scheifinger, H., Stichler, W.: Deuterium excess in
414 precipitation of Alpine regions – moisture recycling, *Isotopes Environ Health Stud*, 44(1), 1-10,
415 <https://doi.org/10.1080/10256010801887208>, 2008.
- 416 Gabrielli, P., Barbante, C., Bertagna, G., Bertò, M., Binder, D., Carton, A., Carturan, L., Cazorzi, F., Cozzi,
417 G., Dalla Fontana, G., Davis, M., De Blasi, F., Dinale, R., Dragà, G., Dreossi, G., Festi, D.,
418 Frezzotti, M., Gabrieli, J., Galos, S.P., Ginot, P., Heidenwolf, P., Jenk, T.M., Kehrwald, N., Kenny,
419 D., Magand, O., Mair, V., Mikhalenko, V., Lin, P.N., Oeggl, K., Piffer, G., Rinaldi, M., Schotterer,
420 U., Schwikowski, M., Seppi, R., Spolaor, A., Stenni, B., Tonidandel, D., Uglietti, C., Zagorodnov,
421 V., Zanoner, T. and Zennaro, P.: Age of the Mt. Ortles ice cores, the Tyrolean Iceman and glaciation
422 of the highest summit of South Tyrol since the Northern Hemisphere Climatic Optimum, *The*
423 *Cryosphere*, 10, 2779-2797, <https://doi.org/10.5194/tc-10-2779-2016>, 2016.
- 424 Haeberli, W., Frauenfelder, R., Käab, A. and Wagner, S.: Characteristics and potential climatic significance
425 of "miniature ice caps" (crest-and cornice-type low-altitude ice archives), *J. Glaciol.*, 50, 129-136,
426 <https://doi.org/10.3189/172756504781830330>, 2004.
- 427 Hoffmann, H., Preunkert, S., Legrand, M., Leinfelder, D., Bohleber, P., Friedrich, R., and Wagenbach, D.:
428 A new sample preparation system for Micro-14C dating of glacier ice with a first application to a
429 high Alpine ice core from Colle Gnifetti (Switzerland), *Radiocarbon*, 60(2), 517-533,
430 <https://doi.org/10.1017/RDC.2017.99>, 2018.



- 431 Huber, C.J., Salionov, D., Burgay, F., Eichler, A., Jenk, T.M., Bjelic, S. and Schwikowski, M.: Molecular
432 reconstruction of organic aerosol composition from a firm core collected at Grand Combin, Swiss
433 Alps, IPICS, Abstract 205, 2022.
- 434 IAEA. <https://www.iaea.org/services/networks/gnip>, last access: 09 May 2023.
- 435 Legrand, M., Preunkert, S., Schock, M., Cerqueira, M., Kasper-Giebl, A., Afonso, J., Pio, C., Gelencsér A.
436 and Dombrowski-Etchevers, I.: Major 20th century changes of carbonaceous aerosol components
437 (EC, WinOC, DOC, HULIS, carboxylic acids, and cellulose) derived from Alpine ice cores, *J.*
438 *Geophys. Res.-Atmos.*, 112, D23S11, <https://doi.org/10.1029/2006JD008080>, 2007.
- 439 Pavlova, P.A., Jenk, T.M., Schmid, P., Bogdal, C., Steinlin, C. and Schwikowski, M.: Polychlorinated
440 biphenyls in a temperate alpine glacier: 1. Effect of percolating meltwater on their distribution in
441 glacier ice, *Environ. Sci. Technol.*, 49(24), 14085-14091, <https://doi.org/10.1021/acs.est.5b03303>,
442 2015.
- 443 Preunkert, S., Legrand, M., and Wagenbach, D.: Sulfate trends in a Col du Dôme (French Alps) ice core:
444 A record of anthropogenic sulfate levels in the European midtroposphere over the twentieth
445 century, *J. Geophys. Res.*, 106 D23, 31,991-32,004, <https://doi.org/10.1029/2001JD000792>, 2001.
- 446 Preunkert, S., Wagenbach, D. and Legrand, M.: A seasonally resolved alpine ice core record of nitrate:
447 Comparison with anthropogenic inventories and estimation of preindustrial emissions of NO in
448 Europe, *J. Geophys. Res.*, 108, D21, 4681, 1-10, <https://doi.org/10.1029/2003JD003475>, 2003.
- 449 Schotterer, U., Stichler, W., and Ginot, P.: The influence of post-depositional effects on ice core studies:
450 examples from the alps, andes, and altai, in: DeWayne Cecil, L., Green, J.R., Thompson, L.G. (eds)
451 *Earth Paleoenvironments: Records Preserved in Mid- and Low-Latitude Glaciers. Developments*
452 *in Paleoenvironmental Research*, vol 9. Springer, Dordrecht. [https://doi.org/10.1007/1-4020-2146-](https://doi.org/10.1007/1-4020-2146-1_3)
453 [1_3](https://doi.org/10.1007/1-4020-2146-1_3), 2004.
- 454 Schwikowski, M., Döscher, A., Gäggeler, H.W. and Schotterer, U.: Anthropogenic versus natural sources
455 of atmospheric sulfate from an Alpine ice core, *Tellus Ser. B Chem. Phys. Meteorol.*, 51, 938-951,
456 <https://doi.org/10.3402/tellusb.v51i5.16506>, 1999a.
- 457 Schwikowski, M., Brüttsch, S., Gäggeler, H.W. and Schotterer, U.: A high-resolution air chemistry record
458 from an Alpine ice core: Fiescherhorn glacier, Swiss Alps, *J. Geophys. Res.*, 104, D11, 13709-
459 13719, <http://dx.doi.org/10.1029/1998JD100112>, 1999b.
- 460 Siegenthaler, U., and Oeschger, H: Correlation of ¹⁸O in precipitation with temperature and altitude, *Nature*,
461 285, 314-317, <https://doi.org/10.1038/285314a0>, 1980.
- 462 Souchez, R.A. and Jouzel, J.: On the isotopic composition in δ D and δ^{18} O of water and ice during freezing,
463 *J. Glaciol.*, 30, 106, 369-372, <https://doi.org/10.3189/S0022143000006249>, 1984.
- 464 Spagnesi, A., Barbaro, E., Feltracco, M., De Blasi, F., Zannoni, D., Dreossi, G., Petteni, A., Notø, H., Lodi,
465 R., Gabrieli, J., Holzinger, R., Gambaro, A., and Barbante, C.: An upgraded CFA – FLC-MS/MS
466 system for the semi-continuous detection of levoglucosan in ice cores, *Talanta*,
467 <https://doi.org/10.1016/j.talanta.2023.124799>, 2023.



468 Steinlin, C., Bogdal, C., Pavlova, P.A., Schwikowski, M., Lüthi, M.P., Scheringer, M., Schmidt P. and
469 Hungerbühler, K.: Polychlorinated Byphenyls in a Temperate Alpine Glacier: 2. Model Results of
470 Chemical Fate Processes, *Environ. Sci. Technol.*, 49, 14092-14100,
471 <https://doi.org/10.1021/acs.est.5b03304>, 2015.

472 Uglietti, C., Zapf, A., Jenk, T. M., Sigl, M., Szidat, S., Salazar, G., and Schwikowski, M.: Radiocarbon
473 dating of glacier ice: overview, optimisation, validation and potential, *The Cryosphere*, 10(6),
474 3091-3105, <https://doi.org/10.5194/tc-10-3091-2016>, 2016.

475 Wagenbach, D., and Geis, K.: The mineral dust record in a high altitude glacier (Colle Gnifetti, Swiss Alps),
476 in: *Paleoclimatology and Paleometeorology: Modern and Past Patterns of Global Atmospheric*
477 *transport*, edited by: Wagenbach, D., and Geis, K. Kluwer Academic Publishers, NATO ASI Series,
478 vol 282, Springer, Dordrecht, 543-564, https://doi.org/10.1007/978-94-009-0995-3_23, 1989.

479 Wagenbach, D., Preunkert, S., Schäfer, J., Jung, W. and Tomadin, L.: Northward transport of Saharan Dust
480 recorded in a deep alpine ice core, in: *Environmental Science and Technology Library*, ENST, vol.
481 11, https://doi.org/10.1007/978-94-017-3354-0_29, 1996.

482 Wagenbach, D., Bohleber, P. and Preunkert, S.: Cold, alpine ice bodies revisited: what may we learn from
483 their impurity and isotope content?, *Geogr. Ann.*, 94(2), 245-263, [https://doi.org/10.1111/j.1468-](https://doi.org/10.1111/j.1468-0459.2012.00461.x)
484 [0459.2012.00461.x](https://doi.org/10.1111/j.1468-0459.2012.00461.x), 2012.

485
486
487
488
489
490
491
492
493
494
495
496
497
498
499
500
501
502
503
504